Clim. Past Discuss., 9, 6345–6373, 2013
www.clim-past-discuss.net/9/6345/2013/
doi:10.5194/cpd-9-6345-2013

Climate of the Past Discussions
Open Access

Modeling of severe persistent droughts over eastern China during the last millennium

Y. Peng[1], C. Shen[2], H. Cheng[3,4], and Y. Xu[5]

[1]Department of Earth Environmental Science, Xi'an Jiaotong University, Xi'an, China
[2]Key Laboratory of Plateau Lake Ecology and Global Change, Yunnan Normal University, Kunming, China
[3]Institute of Global Environmental Change, Xi'an Jiaotong University, Xi'an, China
[4]Department of Geology and Geophysics, University of Minnesota, Minneapolis, USA
[5]Laboratory for Climate Studies, China Meteorological Administration, Beijing, China

Received: 29 September 2013 – Accepted: 8 November 2013 – Published: 20 November 2013

Correspondence to: Y. Peng (youbingpeng@mail.xjtu.edu.cn)

Published by Copernicus Publications on behalf of the European Geosciences Union.

Abstract

We use proxy data and modeled data from 1000 yr model simulations with a variety of climate forcings to examine the occurrence of severe events of persistent drought over eastern China during the last millennium and to diagnose the mechanisms. Results show that the model was able to simulate many aspects of the low-frequency (periods greater than 10 yr) variations of precipitation over eastern China during the last millennium, including most of the severe persistent droughts such as those in the 1130s, 1200s, 1350s, 1430s, 1480s, and the late 1630s–mid-1640s. These six droughts are identified both in the proxy data and in the modeled data and are consistent with each other in terms of drought intensity, duration, and spatial coverage.

Our analyses suggest that monsoon circulation can lock into a drought-prone mode that may last for years to decades and supports the suggestion that generally reduced monsoon in eastern Asia were associated with the land–sea thermal contrast. Study on the wavelet transform and spectral analysis reveals six well-captured events occurred all at the drought stages of statistically significant 15–35 yr timescale. A modeled data intercomparison suggests that solar activity is the primary driver in the occurrence of the 1130s, 1350s, 1480s, and late 1630s–mid-1640s droughts. Although the El-Niño–Southern Oscillation (ENSO) plays an important role in monsoon variability, a temporally consistent relationship between the droughts and SST pattern in the Pacific Ocean could not be found in the model. Our analyses also indicate that large volcanic eruptions play a role as an amplifier in the drought of 1635–1645 and caused the model to overestimate the decreasing trends in summer precipitation over eastern China during the mid-1830s and the mid-1960s.

CPD
9, 6345–6373, 2013

1 Introduction

Drought is a great recurring extreme climate event that strikes eastern China. Due to the significant impacts of climate extremes on economy, society, and environment (Easterling et al., 2000; Changnon et al., 2001; IPCC, 2002), droughts have been received increasing attention in recent years. In particular, severe multiyear droughts, because of their long durations and wide area coverage, can have devastating effects. For example, the most recent drought of this type, which occurred during the 1960s, is the most severe multiyear drought of the late 20th century over eastern China and caused more than 1 million deaths (http://www.intute.ac.uk/hazards/Droughts-timeline.html; Shen et al., 2007).

Based on the instrumental and historical data in China, considerable effort has been made to reveal the occurrence of drought events on temporal scales that range from seasons to years. Work to reconstruct drought status from historical record analysis over eastern China revealed that severe large-scale droughts have occurred many times during the last millennium, with the most severe droughts in the 12–13th and 15–17th centuries and fewer such ones since the middle of the 17th century (Zheng et al., 2006). These efforts have primarily focused on characteristics of droughts – such as their genesis and development, severity, and resulting damages and losses – and elucidating the relationship between drought and temperature (e.g., Wang and Zhao, 1979; Zhang, 1988; Zhang and Crowley, 1989; Yan et al., 1992; Qian et al., 2003, 2012; Shen et al., 2007).

It is also important to understand the causes, and thereby improve predictions, of droughts. The precipitation change over eastern China is mainly driven by the Asian summer monsoon (ASM), which is divided into two strongly nonlinear interacting subsystems: the east Asian summer monsoon (EASM) and the Indian summer monsoon (ISM) (Wang et al., 2001). Wang et al. (2000b) used observational data of years 1951–1996 to study possible causes for drought in northern China, and found that the western Pacific subtropical high and meridional monsoon circulation in the middle latitudes over

CPD
9, 6345–6373, 2013

eastern Asia are responsible for the occurrence of summer rainfall in northern China. On the basis of reconstructions of precipitation variability over large-scale monsoon Asia, together with reconstructions of monsoon variability, it appears that four out of five episodes of "monsoon megadroughts" during the Little Ice Age (LIA) occurred over monsoon Asia within a period of generally reduced monsoon strength in Asia between AD 1300 and 1700 (Sinha et al., 2011b). Several candidate forcing factors that are important and potentially independent mechanisms for monsoon failures have been linked to the occurrence of droughts over eastern China, including solar activity (Liu, 2009; Zhang et al., 2010; Sun, 2012), volcanic eruptions (Xu, 1986; Shen et al., 2007; Peng et al., 2009b; Zhang et al., 2010, 2012), anomalous sea surface temperature such as the El Niño–Southern Oscillation (ENSO; e.g., Huang and Wu, 1989; Liu and Ding, 1992; Zhang and Xue 1994; Lau and Weng, 2000; Li et al., 2005, 2010; Shen et al., 2007) and Pacific Decadal Oscillation (PDO; e.g., Zhu and Yang, 2003; Shen et al., 2006), and anomalous sea level pressure such as North Atlantic Oscillation (NAO; e.g., Sung et al., 2006; Yang et al., 2012; Barriopedro et al., 2012).

The modeling approach, as a powerful tool, allows us to study the characteristics of severe persistent drought during the last millennium and provides important insights into the mechanisms that cause these climate variations. Most general circulation models (GCMs) have often been used to simulate precipitation changes for the region as well as more frequent and extreme departures from mean conditions, including severe droughts, and the related large-scale atmospheric circulation (Seager et al., 2005; Meehl and Hu, 2006; Yu et al., 2013). Based on a 1360 yr control run from a global coupled climate model, Meehl and Hu (2006) linked the megadroughts in the southwestern United States and the Indian monsoon regions, which represent extreme events of naturally occurring multidecadal precipitation variations, to the dominant pattern of multidecadal SST variability in the Indian and Pacific oceans. Another modeling study suggested that variations in solar insolation are the main drivers for the SST anomalies in the Indian Ocean (Polanski et al., 2013). Analysis of the simulations produced by Earth system models indicates that the long-term changes of the east Asia summer

CPD
9, 6345–6373, 2013

monsoon are dominated by the land–sea thermal contrast change (Man et al., 2012), which may be associated with the variations in external radiative forcing (insolation, volcanic aerosol, and greenhouse gases) coupled with the remote impact of the internal dynamics of climate modes in the oceans, such as ENSO and PDO, suggested by other model studies (Liu et al., 2011). However, few works have focused on understanding the occurrence of the severe decadal droughts in China, although studies to date have revealed some extreme persistent drought events over the last thousand years (e.g., Zhang et al., 2005; Zheng et al., 2006; Shen et al., 2007; Qian et al., 2012).

In this study, we will examine the occurrence of severe events of persistent drought over eastern China (east of 105° E, 25–40° N) during the last millennium by combining proxy and modeled data and will explore possible causes for severe persistent drought events using the simulated data.

2 Data and model

The data used in this study include proxy and modeled data of summer precipitation (May–September) over eastern China. The former is a data set of the dryness–wetness index (DWI), a proxy data set of summer rainfall over eastern China from 1470 to 2000 derived from Chinese historical documents and instrumental measurements (CNMA, 1981; Zhang et al., 2003). This index uses five grades (1 – very wet, 2 – wet, 3 – normal, 4 – dry, 5 – very dry) to describe climate conditions. The relative frequencies of five grades – i.e., 10, 25, 30, 25, and 10 % – are defined by observed summer rainfall anomalies (Zhang, 1988; Wang et al., 2000b). Additionally, 1000 yr time series of regional DWI over eastern China (east of approximately 105° E, 25–40° N) reconstructed by Zheng et al. (2006) are also analyzed. This data set with 10 yr time resolution is also derived from Chinese historical documents.

Modeled data are four 1000 yr simulations of CCSM2.0 developed by the National Center for Atmospheric Research (NCAR; Kiehl and Gent, 2004). The model comprises four components of the climate system: the atmosphere, ocean, land surface,

CPD
9, 6345–6373, 2013

and sea ice. These components are linked via a flux coupler without flux corrections. The atmospheric component is a primitive equation model with T31 in horizontal resolution (~ 3.75° in latitude and longitude) and 26 hybrid-coordinate levels in the vertical. The land component has the same horizontal grid as the atmosphere and includes 5 different surface types (glacier, lake, wetland, urban, and vegetated) with 4 to 16 different vegetation types. The ocean component is the NCAR implementation of the POP (Parallel Ocean Program; Smith and Gent, 2002) and has a longitudinal resolution of ~ 3.6° and variable latitudinal resolutions of ~ 1.8° and up to ~ 0.9° in the tropics. The sea-ice component is a dynamic–thermodynamic model with the same horizontal grid as the ocean component. Four simulations including a control run, a run with orbital and solar forcing, a run with orbital and volcanic forcing, and another run with full forcing are conducted (Peng et al., 2009a). Forcing time series used in runs include the global and seasonal change of the orbital insolation (Berger, 1978), solar variation and volcanic eruption (Crowley et al., 2003), and greenhouse gases (Ammann et al., 2007).

3 Defining an index of the eastern Asian land–sea heat source difference

The occurrence of the EASM variability is a consequence of the atmospheric response to the diabatic heating between the ocean and the land (Li and Yanai, 1996). Sun et al. (2002) found the EASM region to be not only under the effect of zonal but also meridional land–sea thermal difference. Sun et al. (2000) defined an index of land–sea thermal difference (ILSTD) that includes zonal and meridional land–sea thermal difference. Zonal thermal difference is defined as surface temperature difference between eastern China (the land at 27–35° N and east of 105° E) and the northwestern Pacific (15–30° N, 120–150° E). Meridional thermal difference is defined as surface temperature difference between southern China (the land south of 27° N and east of 105° E) and the South China Sea (5–18° N, 105–120° E). The zonal thermal difference accounts for 80 % of the land–sea thermal difference, and the meridional thermal difference accounts for 20 %.

CPD
9, 6345–6373, 2013

4 Results

Figure 1 shows the precipitation variation in proxy data and full-forcing modeled data over eastern China during the last 1000 yr. Two DWI series and the modeled data have all been subjected to a 10 yr running mean to remove the effects of interannual variability and to retain variability on timescales of just under a decade and longer. The general impression from the figure is that the simulation produces a time temporal variability similar to that observed in proxy data except during the periods of 1360–1420, the 16th century, and after 1820. We note the long poor matches between model and proxy data occur in the last century. One possible reason is that our model overestimates the response to increasing greenhouse gas forcing. The greenhouse-gas-induced increasing of summer precipitation over eastern China (Peng et al., 2009a) is largely overwhelming the other forcings. An alternative is that a number of potentially important forcings are not considered in the simulations studied here, such as the climate effects of black carbon aerosols (Xu, 2001; Menon et al., 2002) and human-induced land cover changes (Fu, 2002, 2003). Both the model and proxy data show that the variability of summer precipitation over eastern China exhibits fluctuations on the decadal and centennial timescales. On the centennial timescales, both the simulation and reconstruction show that the 12th, 15th, 16th, 17th, and 19th centuries encountered more occurrences of drought conditions than 11th, 13th, 14th, and 18th centuries, while the model underestimates the frequency of droughts in the 20th century due to the reasons mentioned above.

Here, we focus on the decadal timescale droughts. Severe decadal droughts in the model are defined as periods with a precipitation anomaly of at least widespread (over eastern China, east of 105° E, 25–40° N), persistent (more than 5 yr), and great precipitation anomaly (severe drought). To identify these events, we used −0.43 as the threshold to classify the severity of severe, based on the normalized time series of 10 yr running mean of precipitation for eastern China, meaning that the probability of drought occurrence is 10 % (Solomon et al., 2007a). This approach of defining drought

CPD
9, 6345–6373, 2013

years was also employed by Yu et al. (2013). The same approach is also applied to identify the severe decadal drought in the proxy data. We selected the periods of at least five consecutive years with a precipitation anomaly of at least 1.28 times the standard deviation lower than the mean value based on the 1000 yr DWI series, meaning that the probability of drought is 10 %. In this classification, the proxy data show that 10 severe decadal droughts have occurred during the last millennium, and most of them are produced by the model, i.e., the droughts of the 1130s, 1200s, 1350s, 1430s, 1480s, and the late 1630s–mid-1640s (Table 1). However, the model underestimates the severity and length of the 1070s and 1170s droughts and misses two droughts in the 16th century detected in the proxy data. Figure 1 and Table 1 also reveal some rather peculiar model behavior during the early 1000s, mid-1410s, mid-1830s, and mid-1960s. Compared to the proxy data, it is obvious that the model overestimates the drought conditions during the period from 1000 to 1004, which could be attributed to the initial starting condition. Although the proxy data show a very wet period occurring from 1416 to 1422 over eastern China, severe drought conditions are found using other proxy data in other regions over monsoon Asia, such as in India (Sinha et al., 2007), central China (Zhang et al., 2008), and southern Vietnam (Buckley et al., 2010). This spatiotemporal pattern during the 1410s revealed by the proxy data over monsoon Asia is associated with the warmer tropical Indian and western Pacific oceans as well as the cooler tropical eastern Pacific Ocean (Graham et al., 2010), which the model cannot produce (not shown). Although significant decreases in summer precipitation over eastern China during the 1830s and 1960s are observed in the proxy data, the climate in these two periods was still considered to be at wet or normal conditions. Thus it seems the model overestimates the decreasing trends in summer precipitation in the periods of the 1830s and 1960s. Next, these six well-captured droughts that we have mentioned above will be focused on.

Figure 2 shows maps of the model summer precipitation anomalies for six well-captured droughts. For six droughts, dry conditions are all widespread across the entire regions of eastern China, but with different drought centers. In the proxy data, the

CPD
9, 6345–6373, 2013

great drought during the period of 1482–1489 stretched over most regions over eastern China (Fig. 2g), with the most severe conditions located in northern China (Sun et al., 2012). The model produces this major drought, with the locations of maximum drought in the middle–lower Yangtze River valley (Fig. 2e). In the proxy reconstructions (Shen et al., 2007; Cook et al., 2010), between 1638 and 1641 the entire eastern China experienced drought, with the driest conditions centred in the north of China (Fig. 2h). The model produces this widespread drought, as well as the increased severity in the north of China (Fig. 2f). Thus, in terms of drought intensity, duration, and spatial coverage, these six droughts over eastern China revealed by our model are consistent with the results of proxy data. Among the six well-captured droughts, the first three appeared in the warm period of Medieval Climate Anomaly (MCA), whereas the other three occurred in the cold period of LIA. The question here is, since they happened in different climatic background, which natural forcing causes these severe persistent drought events with long periods of time, great intensity, and extensive coverage.

Anomalies of summer 850 hPa winds during the six well-captured droughts are shown in Fig. 3. They are characterized by the weakening of the 850 hPa southwesterly winds over eastern China, indicating a generally weaker EASM in these droughts. This result is consistent with the previous proxy study from reconstructions of precipitations and monsoon variability in monsoon Asia, which indicates a weak ASM during the four megadroughts that occurred in the LIA (Sinha et al., 2011b). The model response is also consistent with the modeling study, which shows that a weak EASM often assumes an in-phase rainfall decrease of extratropical and subtropical precipitation over eastern China (Liu et al., 2011). For changes of land–sea thermal contrast that lead to the EASM monsoon changes suggested by Man et al. (2012), we used an index of land–sea thermal difference (ILSTD) that describes its zonal and meridional strength responsible for EASM circulation (Sun et al., 2000) in order to study its relation to the east Asian monsoon circulation and the summer rainfall over China during these droughts (Fig. 4). Results show that the land–sea thermal difference is generally strong during the MCA, weak during the LIA, and strong again after 1700. The results

CPD
9, 6345–6373, 2013

are consistent with the reconstructions of monsoon variability from the speleothem oxygen isotope records in Wanxiang Cave (Zhang et al., 2008) and Dongge Cave (Wang et al., 2005) in China, showing that the long-term changes of EASM are dominated by the land–sea thermal contrast change. We observed six droughts that occurred in the periods following remarkably weak index corresponding to the weak EASM, suggesting that the weak summer monsoon during these droughts may be driven by the changes of land–sea thermal contrast. The internal dynamics of climate modes in the oceans, such as ENSO and PDO, and the external forcing of effective solar radiation would contribute to the thermal changes that correspond to the weak EASM and hence cause these severe decadal droughts.

To examine possible causes of these monsoon failures (droughts), first of all, wavelet analysis is used to investigate how the dominant timescales of drought variability change with time. Study on the wavelet transform in the 10 yr running average precipitation series has detected the cycle periods. Figure 5 shows the wavelet coefficients for the timescales 8–128 yr over the period during the last thousand years. Bidecadal variability (15–35 yr) exists throughout the last millennium, and it is clear that for all six well-captured droughts and the elevated aridity in the mean, bidecadal variability is evident, with some statistically significant strength also in the multidecadal bands (50–70 yr). The presence of a bidecadal rhythm in eastern China precipitation variability has been noted in the past from observations, proxy records, and other simulation data over eastern China (Jiang et al., 1997; Zhu et al., 2001; Qi et al., 2001; Qian et al., 2001, 2003, 2012; Liu, 2011; Shen et al., 2009). To examine possible attributions of the 15–35 yr oscillation, we also conduct spectral analysis on the modeled summer precipitation from the control run and solar run. As shown by Fig. 6d–f, the bidecadal peaks in the 15–35 yr variability revealed in the control run match those in the solar forcing run, which is consistent with the length of cycles in oceanic records such as the PDO, with fluctuations at periodicities of 15 yr and 20–30 yr, and with NAO fluctuations at periodicities of 20 yr, and similar to solar radiation cycles of 22 yr in the Hale solar magnetic cycle, suggesting that they could be associated with solar activity and

CPD
9, 6345–6373, 2013

internal variability of the climate system. Thus, it strengthens the argument we mentioned above that solar activity and the internal variability of the climate system may be the drivers of these severe persistent drought occurrences.

As shown by Fig. 7, a temporally consistent relationship between the droughts and SST pattern in the Pacific Ocean could not be found in the model. There is an El Niño-like SST pattern occurring during the droughts of 1133–1140 and 1482–1489; a La Niña-like SST pattern occurring during the droughts of 1356–1360, 1439–1444, and 1635–1645; and a neutral pattern occurring during the droughts of 1204–1210. By comparing a series of proxy records that reflect changes in El Niño frequency or the mean state of ENSO in the tropical Pacific, Sinha et al. (2010) also found that there is no conclusive evidence to suggest that the megadroughts in monsoon Asia were associated with anomalous sea surface temperature anomalies that were solely the result of ENSO-like variability in the tropical Pacific. As it is limited by the ability of simulating the internal modes of variability, the model does not simulate a persistent negative PDO at the episode of the first two droughts during MCA, as suggested by a 1000 yr tree-ring-based reconstruction of the PDO (MacDonald and Case, 2005; Fig. 4). Figure 6b shows the precipitation time series over eastern China during the last millennium in the solar forcing run and the severe persistent drought events that were identified in the same way in the full forcing run. Over the last thousand years, the effective solar radiation forcing has experienced six periods of significant minimum; these occurred during the periods of 950–1150, 1250–1350, 1400–1550, 1645–1715, and 1790–1830, and around 1900. It is of interest to observe that all the severe decadal droughts identified in the solar forcing run occurred following the minimum effective solar radiation forcing except that during the Dalton Minimum (1790–1830). The droughts of the 1130s, 1350s, 1480s, and the late 1630s–mid-1640s detected in the full forcing run are also identified in the solar forcing run, albeit with frequent phase shifts of severe years or so, indicating that solar activity plays a dominant role in these droughts. The drought of the 1430s is not identified in the solar forcing run, whereas the most severe sustained drought condition was observed in the period between the 1440s and 1450s in

CPD
9, 6345–6373, 2013

the control run (Fig. 6a). However, that the agreement in timing between droughts in the full forcing run and control run matches up is simply a coincidence. The drought of 1200s was not detected in both the control and solar forcing runs, which is not unexpected since a grand episode of higher solar activity appeared during this time and the SST pattern over the Pacific Ocean in the model during this drought interval was generally neutral, suggesting that other factors caused the drought events during the period from 1204 to 1210.

One other possible forcing responsible for drought events occurring over eastern China is volcanic eruption. Shen et al. (2007) suggested that large volcanic eruptions could trigger exceptional droughts over eastern China. In our previous work (Peng et al., 2009b), an analysis of response of summer precipitation over eastern China to large volcanic eruptions showed that summer precipitation over eastern China significantly decreases in the year with lowest reduction in solar irradiance and the year after. As shown in Fig. 8, there is no volcanic activity during the drought of 1430s and 1200s and wet conditions were produced in the volcanic forcing run. Thus some other important climate modes, which are often connected with extreme climate events, may have caused the drought of the 1200s, and future research into this drought is clearly warranted. We note that during the drought of 1635–1645 – which is the most severe sustained drought for eastern China in proxy data and the longest drought in modeled data (Table 1) – one large volcanic eruption occurred. The eruption of Mt. Parker in the Philippines in 1641 caused the lowest reduction in solar irradiance of $-15.6\,\mathrm{W\,m^{-2}}$ in the next year (Fig. 8a), indicating volcanic eruption may play a role as an amplifier of this event. In addition, explosive volcanism may also play an important role in causing the other two drought events of 1834–1841 and 1964–1969 in the full forcing run, which could not be identified in the solar forcing run. One or more colossal volcanic eruption occurred during these two events: for example, Cosiguina in Nicaragua in 1835 caused the lowest reduction value of $-10.4\,\mathrm{W\,m^{-2}}$ in the volcanic eruption year, and Mt. Agung in Indonesia in 1963 caused the lowest reduction value of $-6\,\mathrm{W\,m^{-2}}$ in the next year (Fig. 8a). The responses to these eruptions are evident events in the full

CPD
9, 6345–6373, 2013

forcing run that caused more than a 1-σ decrease in precipitation in 1644, 1835, and 1964 and more than a 2-σ decrease in 1643, which is large enough to explain the observed droughts. Our previous study (Peng et al., 2009b) suggested that this reduction of summer precipitation over eastern China could be attributed to a weakening of summer monsoon and a decrease of moisture vapor over tropical oceans caused by large volcanic eruptions. As shown in Fig. 8b, the 1830s and 1960s droughts detected in the full forcing run are captured well in the volcanic forcing run, which strengthens the argument that these two overestimated events are forced by volcanic eruptions. Thus, our model overestimates the influences of volcanic eruptions on summer precipitation over eastern China during these two periods.

5 Discussion and conclusions

We have presented results from model simulations of the severe persistent droughts over eastern China during the last millennium. The CCSM2.0 forced by a variety of climate forcings during the last millennium simulates many aspects of the observed precipitation variations with periods of 10 yr or longer over eastern China except during the periods of 1360–1420, the 16th century, and after 1820. On the decadal timescales, eastern China experienced 10 major multiyear droughts during the last thousand years. Although 2 great droughts in the 16th century are missed by the model and the reason why is still not clear, the model does an impressive job at capturing 6 of these 10 droughts, i.e., the droughts of the 1130s, 1200s, 1350s, 1430s, 1480s, and the late 1630s–mid-1640s. In particular, in terms of spatial coverage, these six persistent drought events in the model are consistent with the results of the proxy data.

Our analysis suggests that the case for repeated occurrences of severe persistent droughts identified both in proxy and modeled data is sufficiently compelling to suggest that monsoon circulation can lock into a drought-prone mode that may last for years to decades, and supports the suggestion that reduced monsoon in eastern Asia was generally associated with the land–sea thermal contrast. The wavelet analysis of the

CPD
9, 6345–6373, 2013

summer precipitation variability over eastern China reveals that bidecadal variability (15–35 yr) exists and was prominent throughout the last millennium. It dominates in the arid period of six well-captured droughts. A model–data intercomparison suggests that the bidecadal oscillation could be associated with internal variability of the climate system and the solar activities. It indicates that variations in solar insolation coupled with the remote impact of the internal dynamics of climate modes are some of the major drivers leading to persistent server drought over eastern China.

While the climate dynamics associated with the ENSO and its low-frequency counterpart PDO have been shown to exert considerable, albeit intermittent, influences on monsoon rainfall over eastern China during the instrumental period, our analysis of simulation does not reveal a clear role of the ENSO in causing these severe decadal droughts. Nonetheless, it would be premature to discount the role of the tropical Pacific until additional unambiguous high-resolution ENSO sensitive proxy records become available, and more climate model experiments should be performed using the new version of CCSM, which has largely eliminated these biases in the simulations of ENSO in CCSM2.0. The solar activities are the ultimate driver of four severe persistent droughts over eastern China, as evidenced by the ability of the model to reproduce these when only the solar forcing is specified. However, the factor that caused the droughts of the 1200s and 1430s is still not clear. Volcanic eruptions play a role as an amplifier during the periods of 1635–1645, 1834–1841, and 1964–1969.

Due to the uncertainties in the forcing reconstructions and the models of chaotic components of internal variability, models could not reproduce the exact variability registered in the proxy data. Furthermore, drought events that occurred over eastern China may have resulted from a series of complex climatic processes that are much more complicated than those we discussed here. Thus, the results presented here only allow for a tentative conclusion. If the modeling results regarding the relationship between solar radiation forcing and drought events hold up, then the precursor of the future eruption of the Changbaishan Tianqi volcano in northeastern China and the fact that the Sun might enter an extended period of low activity similar to the Maunder

CPD
9, 6345–6373, 2013

Minimum in the 17th century will lead to a greater prevalence of drought over eastern China in the future.

Acknowledgements. This work is supported by the National Basic Research Program of China (grant # 2013CB955904, 2013CB955902) and the National Natural Science Foundation of China (grant # 41230524).

References

Ammann, C., Joos, F., Schimel, D., Otto-Bliesner, B., and Tomas, R.: Solar influence on climate during the past millennium: results from transient simulations with the NCAR Climate System Model, P. Natl. Acad. Sci. USA, 104, 3713–3718, 2007.

Anchukaitis, K., Buckley, B., Cook, E., Cook, B., D'Arrigo, R., and Ammann, C.: Influence of volcanic eruptions on the climate of the Asian monsoon region, Geophys. Res. Lett., 37, 22703, doi:10.1029/2010GL044843, 2010.

Barriopedro, D., Gouveia, C., Trigo, R., and Wang, L.: The 2009/10 drought in China: possible causes and impacts on vegetation, J. Hydrometeorol., 13, 1251–1267, 2012.

Berger, A.: Long-term variations of daily insolation and quaternary climatic changes, J. Atmos. Sci., 35, 2362–2367, 1978.

Boer, G., Flato, G., and Ramsden, D.: A transient climate change simulation with greenhouse gas and aerosol forcing: projected climate for the 21st century, Clim. Dynam., 16, 427–450, 2000.

Buckley, B., Palakit, K., Duangsathaporn, K., Sanguantham, P., and Prasomsin, P.: Decadal scale droughts over northwestern Thailand over the past 448 years: links to the tropical Pacific and Indian Ocean sectors, Clim. Dynam., 29, 63–71, 2007.

Buckley, B., Anchukaitis, K., Penny, D., Fletcher, R., Cook, E., Sano, M., Nam, L., Wichienkeeo, A., Minh, T., and Hong, T.: Climate as a contributing factor in the demise of Angkor, Cambodia, P. Natl. Acad. Sci., 107, 6748–6752, 2010.

Changnon, S., Changnon, J., and Hewings, G.: Losses caused by weather and climate extremes: a national index for the United States, Phys. Geogr., 22, 1–27, 2001.

CNMA (Chinese National Meteorological Administration): Yearly Charts of Dryness/Wetness in China for the Last 500-Year Period, Chinese Cartographic Publishing House, Beijing, 1981.

Collins, M.: El Niño – or La Niña like climate change?, Clim. Dynam., 24, 89–104, 2005.

CPD
9, 6345–6373, 2013

Cook, E., Anchukaitis, K., Buckley, B., D'Arrigo, R., Jacoby, G., and Wright, W.: Asian monsoon failure and megadrought during the last millennium, Science, 328, 486–489, 2010,
Crowley, T., Baum, S., Kim, K., Hegerl, G., and Hyde, W.: Modelling ocean heat content changes during the last millennium, Geophys. Res. Lett., 30, 1932, doi:10.1029/2003GL017801, 2003.
Easterling, D., Meehl, G., Parmesan, C., Changnon, S., Karl, T., and Mearns, L.: Climate extremes: observations, modeling, and impacts, Science, 289, 2068–2074, 2000.
Fu, C.: Can human induced land-cover change modify the monsoon system?, in: Challenges of a Changing Earth, edited by: Steffan, W., Jager, J., Carson, W. J., and Bradshaw, C., Springer, Berlin, 133–136, 2002.
Fu, C.: Impacts of human-induced land cover change on East Asia monsoon, Global Planet. Change, 37, 219–229, 2003.
Graham, N., Ammann, C., Cobb, K., Fleitmann, D., and Lutherbacher, J.: Support for global climate reorganization during the "Medieval Climate Anomaly", Clim. Dynam., 37, 1217–1245, 2011.
Huang, R. and Wu, Y.: The influence of ENSO on the summer climate change in China and its mechanism, Adv. Atmos. Sci., 6, 21–32, 1989.
IPCC: Workshop report of Intergovernmental Panel on Climate Change, in: Workshop on Changes in Extreme Weather and Climate Events, Beijing, 107 pp., 2002.
Jang, J., Zhang, D., and Klaus, F.: Historic climate variability of wetness in East China (960–1992): a wavelet analysis, Int. J. Climatol., 17, 969–981, 1997.
Kiehl, J. and Gent, P.: The Community Climate System Model, version 2, J. Climate, 17, 3666–3682, 2004.
Lau, K. and Weng, H.: Coherent modes of global SST and summer rainfall over China: an assessment of the regional impacts of the 1997–98 El Niño, J. Climate, 14, 1294–1308, 2000.
Li, C. and M. Yanai.: The onset and interannual variability of the Asian summer monsoon in relation to land-sea thermal contrast, J. Climate, 9, 358–375, 1996.
Li, H., Dai, A., Zhou, T., and Lu, J.: Response of East Asian summer monsoon to historical SST and atmospheric forcing during 1950–2000, Clim. Dynam., 34, 501–514, 2010.
Li, Q., Yang, S., Kousky, V., Higgins, R., Lau, K., and Xie, P.: Features of cross-pacific climate shown in the variability of China and US precipitation, Int. J. Climatol., 25, 1675–1696, 2005.

CPD
9, 6345–6373, 2013

Lin, X. and Yu, S.: Evidence of a 22-year cycle of drought in China related to the Hale solar cycle, J. Appl. Meteor. Sci., 1, 43–50, 1987.
Liu, J., Wang, B., Wang, H., Kuang, X., and Ti, R.: Forced response of the East Asian summer rainfall over the past millennium: results from a coupled model simulation, Clim. Dynam., 36, 323–336, 2011.
Liu, Y. and Ding, Y.: Influence of El Niño events on weather and climate in China, Acta. Meteorol. Sin., 6, 117–131, 1992.
Luo, L. and Wood, E.: Monitoring and predicting the 2007 U.S. drought, Geophys. Res. Lett., 34, 22702, doi:10.1029/2007GL031673, 2007 .
Man, W., Zhou, T., and Johann, H.: Simulation of the east Asian summer monsoon during the last millennium with the MPI Earth System Model, J. Climate, 25, 7852–7866, 2012.
Meehl, G. and Hu, A.: Megadroughts in the Indian monsoon region and southwest North America and a mechanism for associated multidecadal Pacific sea surface temperature anomalies, J. Climate, 19, 1605–1623, 2006.
Menon, S., Hansen, J., Nazarenko, L., and Luo, Y.: Climate effects of black carbon aerosols in China and India, Science, 297, 2250–2253, 2002.
Peng, Y., Xu, Y., and Jin, L.: Climate changes over eastern China during the last millennium in simulations and reconstructions, Quatern. Int., 208, 11–18, 2009a.
Peng, Y., Shen, C., Wang, W., and Xu, Y.: Response of summer precipitation over eastern China to large volcanic eruptions, J. Climate, 23, 818–824, 2009b.
Polanski, S., Fallah, B., Prasad, S., and Cubasch, U.: Simulation of the Indian monsoon and its variability during the last millennium, Clim. Past Discuss., 9, 703–740, doi:10.5194/cpd-9-703-2013, 2013.
Qian, W., Hu, Q., Zhu, Y., and Lee, D.: Centennial-scale dry-wet variation in east Asia, Clim. Dynam., 21, 77–89, 2003.
Qian, W., Shan, X., Chen, D., Zhu, C., and Zhu, Y.: Droughts near the northern fringe of the east Asian summer monsoon in China during 1470–2003, Climatic Change, 110, 373–383, 2012.
Seager, R., Kushnir, Y., Herweijer, C., Naik, N., and Velez, J.: Modeling of tropical forcing of persistent droughts and pluvials over western North America: 1856–2000, J. Climate, 18, 4065–4088, 2005.

CPD
9, 6345–6373, 2013

Shen, C., Wang, W., Gong, W., and Hao, Z.: A pacific decadal oscillation record since 1470 AD reconstructed from proxy data of summer rainfall over Eastern China, Geophys. Res. Lett., 33, L03702, doi:10.1029/2005GL024804, 2006.

Shen, C., Wang, W., Hao, Z., and Gong, W.: Exceptional drought events over eastern China during last five centuries, Climatic Change, 85, 453–471, 2007.

Sinha, A., Cannariato, K., Stott, L., Cheng, H., Edwards, R., Yadava, M., Ramesh, R., and Singh, I.: A 900-year (600 to 1500 A.D.) record of the Indian summer monsoon precipitation from the core monsoon zone of India, Geophys. Res. Lett., 34, L16707, doi:10.1029/2007GL030431, 2007.

Sinha, A., Stott, L., Berkelhammer, M., Cheng, H., Lawrence Edwards, R., Buckley, B., Aldenderfer, M., and Mudelsee, M.: A global context for megadroughts in monsoon Asia during the past millennium, Quaternary Sci. Rev., 30, 47–62, 2011.

Smith, R. and Gent, P.: Reference Manual for the Parallel Ocean Program (POP); Ocean Component of the Community Climate System Model (CCSM-2), available at: http://www.ccsm.ucar.edu/models/ccsm2.0.1/pop/ (last access: 18 November 2013), 2002.

Solomon, S., Qin, D., Manning, M., Alley, R., Berntsen, T., Bindoff, N., Chen, Z., Chidthaisong, A., Gregory, J., Hegerl, G., Heimann, M., Hewitson, B., Hoskins, B., Joos, F., Jouzel, J., Kattsov, V., Lohmann, U., Matsuno, T., Molina, M., Nicholls, N., Overpeck, J., Raga, G., Ramaswamy, V., Ren, J., Rusticucci, M., Somerville, R., Stocker, T., Whetton, P., Wood, R., and Wratt, D.: Technical summary, in: Climate Change 2007: The Physical Science Basis. Contribution of Working Group I to the Fourth Assessment Report of the Intergovernmental Panel on Climate Change, edited by: Solomon, S., Qin, D., Manning, M., Chen, Z., Marquis, M., Averyt, K., Tignor, M., and Miller, H., Cambridge University Press, Cambridge, UK and New York, NY, USA, 2007.

Sung, M., Kwon, W., Baek, H., Boo, K., Lim, G., and Kug, J.: A possible impact of the North Atlantic Oscillation on the East Asian summer monsoon precipitation, Geophys. Res. Lett., 33, L21713, doi:10.1029/2006GL027253, 2006.

Sun, J. and Liu, Y.: Tree ring based precipitation reconstruction in the south slope of the middle Qilian Mountains, northeastern Tibetan Plateau, over the last millennium, J. Geophys. Res., 117, D08108, doi:10.1029/2011JD017290, 2012.

Sun, X., Chen, L., and He, J.: Index of land-sea thermal differences and its relation to interannual variation of summer circulation and rainfall over East Asia, Acta Meteorol. Sin., 60, 164–172, 2002.

CPD
9, 6345–6373, 2013

Svoboda, M., LeComte, D., Hayes, M., Heim, R., Gleason, K., Angel, J., Rippey, B., Tinker, R., Palecki, M., Stooksbury, D., Miskus, D., and Stephens, S.: An introduction to the drought monitor, B. Am. Meteorol. Soc., 83, 1181–119, 2002.

Wang, B., Wu, R., and Lau, K.: Interannual variability of the Asian summer monsoon: contrasts between the Indian and the Western North Pacific–East Asian Monsoon, J. Climate, 14, 4073–4090, 2001.

Wang, S. and Zhao, Z.: An analysis of historical data of droughts and floods in the last 500 years in China, Acta Geogr. Sin., 34, 329–341, 1979.

Wang, S., Ye, J., and Qian, W.: Predictability of drought in China, in: Drought, a Global Assessment, edited by: Wilhite, D. A., Routledge, London, 100–112, 2000.

Wang, Y., Cheng, H., Edwards, R., He, Y., Kong, X., An, Z., Wu, J., Kelly, M., Dykoski, C., and Li, X.: The Holocene Asian monsoon: links to solar changes and North Atlantic climate, Science, 308, 854–857, 2005.

Xu, Q.: The abnormal weather of China for summer 1980 and its relationship with the volcanic eruptions of Mount St. Helens, Acta Meteorol. Sin., 44, 426–432, 1986.

Xu, Q.: Abrupt change of the mid-summer climate in central east China by the influence of atmospheric pollution, Atmos. Environ., 35, 5029–5040, 2001.

Yan, Z.: A primary analysis of the process of the 1960s northern hemispheric summer climatic jump, Chinese J. Atmos. Sci., 16, 111–119, 1992.

Yan, Z., Ye, D., and Wang, C.: Climatic jumps in the flood/drought historical chronology of Central China, Clim. Dynam., 6, 153–160, 1992.

Yang, J., Gong, D., Wang, W., Hu, M., and Mao, R.: Affiliation, extreme drought event of 2009/2010 over southwestern China, Meteorol. Atmos. Phys., 115, 173–184, 2012.

Yu, G., Sauchyn, D., and Li, Y.: Drought changes and the mechanism analysis for the North American Prairie, J. Arid Land, 5, 1–14, 2013.

Zhang, D.: The method for reconstruction of the dryness/wetness series in China for the last 500 years and its reliability, in: The Reconstruction of Climate in China for Historical Times, edited by: Zhang, J., Science Press, Beijing, 18–31, 1988.

Zhang, D.: Severe drought events as revealed in the climate records of China and their temperature situations over the last 1000 years, Acta Meteorol. Sin., 19, 485–491, 2005.

Zhang, D. and Liang, Y.: A long lasting and extensive drought event over China in 1876–1878, Adv. Atmos. Sci., 1, 91–99, 2010.

CPD
9, 6345–6373, 2013

Zhang, D. and Xue, Z.: Relationship between El Niño and precipitation patterns in China since 1500 AD, J. Appl. Meteor. Sci., 5, 168–175, 1994.
Zhang, D., Li, X., and Liang, Y.: Supplement of yearly charts of dryness/wetness in China for the last 500-year period, 1993–2000, J. Appl. Meteor. Sci., 14, 379–389, 2003.
Zhang, D., Blender, R., and Fraedrich, K.: Volcanoes and ENSO in millennium simulations: global impacts and regional reconstructions in East Asia, Theor. Appl. Climatol., 111, 437–454, 2013.
Zhang, J. and Crowley, T. J.: Historical climate records in China and reconstruction of past climates (1470–1970), J. Climate, 2, 833–849, 1989.
Zhang, P., Cheng, H., Edwards, R., Chen, F., Wang, Y., Yang, X., Liu, J., Tan, M., Wang, X., Liu, J., An, C., Dai, Z., Zhou, J., Zhang, D., Jia, J., Jin, L., and Johnson, K.: A test of climate, sun, and culture relationships from an 1810-year Chinese cave record, Science, 322, 940–942, 2008.
Zheng, J., Wang, W., and Ge, Q.: Precipitation variability and extreme events over eastern China during the past 1500 years, Terr. Atmos. Ocean. Sci., 17, 579–592, 2006.
Zhu, Y. and Yang, X.: Relationships between pacific decadal oscillation (PDO) and climate variability in China, Acta Meteorol. Sin., 61, 641–653, 2003.

CPD
9, 6345–6373, 2013

Table 1. Severe decadal droughts over eastern China during the last millennium are identified in proxy and simulated data. Bold-faced years are the droughts captured by both the proxy and simulated data.

Century	Droughts in the 1000 yr DWI series (mean value)	Droughts in the simulation (mean value)
1000–1099	– (−0.41)	1000–1004 (−0.63)
	1069–1078 (−1.85)	– (−0.23)
1100–1199	**1131–1146 (−1.89)**	**1133–1140 (−0.63)**
	1175–1180 (−1.58)	– (−0.06)
1200–1299	**1201–1217 (−1.55)**	**1204–1210 (−0.67)**
1300–1399	**1354–1359 (−1.56)**	**1356–1360 (−0.53)**
1400–1499	– (2.0)	1416–1422 (−0.63)
	1433–1440 (−1.69)	**1439–1444 (−0.56)**
	1482–1490 (−1.7)	**1482–1489 (−0.79)**
1500–1599	1524–1529 (−1.55)	– (0.32)
	1584–1588 (−1.69)	– (0)
1600–1699	**1635–1642 (−2.35)**	**1635–1645 (−0.58)**
1700–1799	–	–
1800–1899	– (0.52)	1834–1841 (−0.56)
1900–1999	– (0)	1964–1969 (−0.52)

CPD
9, 6345–6373, 2013

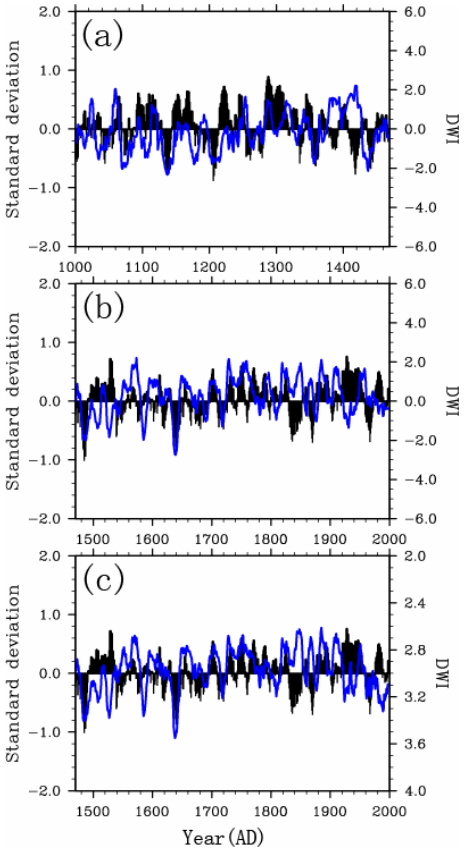

Fig. 1. The summer precipitation anomaly (May–September) from the modeled data (black bars) and DWI from the proxy data (blue curve) of Zheng et al. (2006) over eastern China during the last 1000 yr **(a, b)**.**(c)** Same as **(b)** but from the proxy data of Zhang et al. (2003) during the last 530 yr. All data are 10 yr running averages.

CPD
9, 6345–6373, 2013

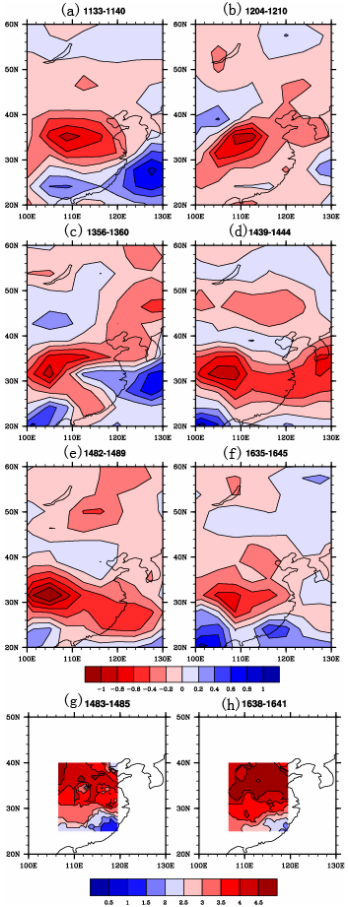

Fig. 2. Modeled precipitation anomalies of the six well-captured droughts **(a–f)** and the last two regional droughts identified from the historical records from the periods 1483–1485 **(g)** and 1638–1641 **(h)**.

CPD
9, 6345–6373, 2013

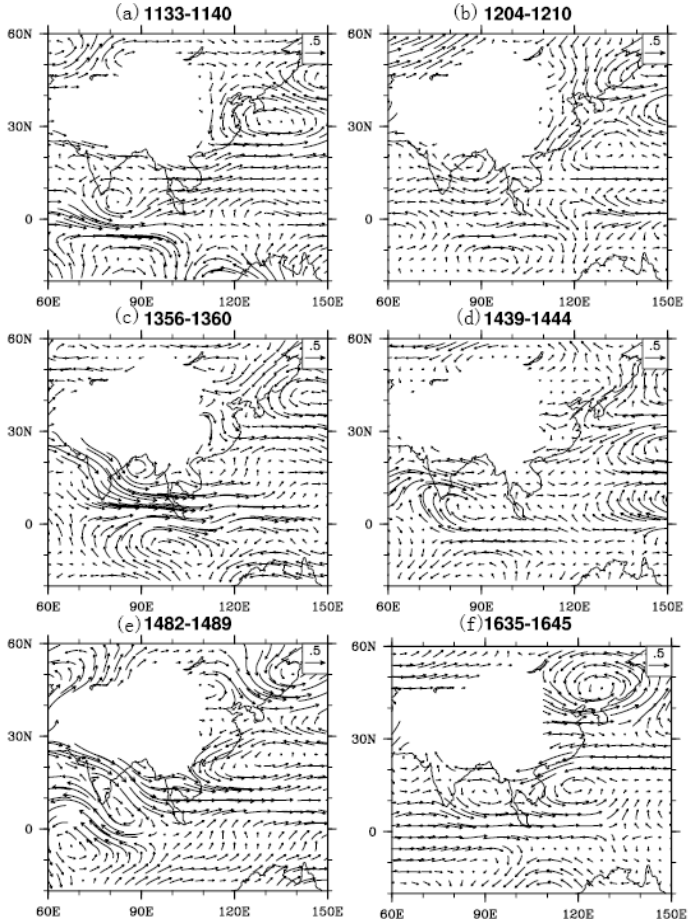

Fig. 3. Same as Fig. 2 but for the wind at the level of 850 hpa for the six well-captured droughts.

CPD
9, 6345–6373, 2013

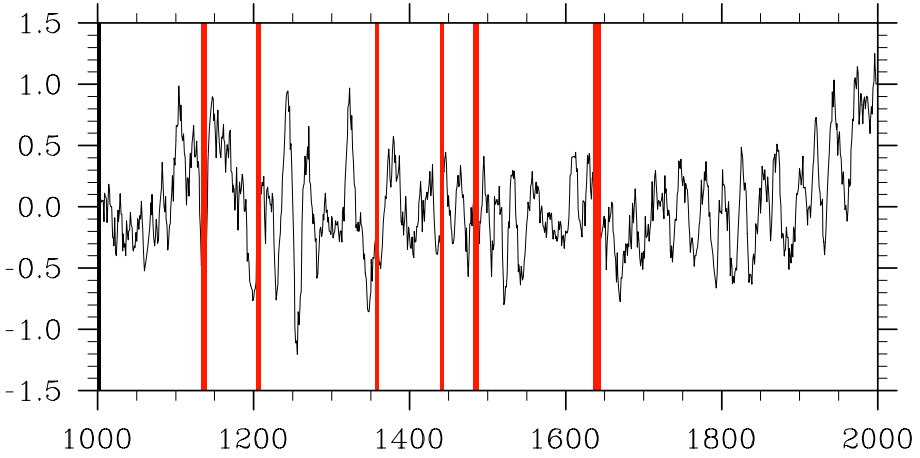

Fig. 4. The 10 yr running mean time series of standardized anomaly variations for the index of land–sea thermal difference (ILSTD). Six well-captured severe decadal droughts are shown with red bars.

CPD
9, 6345–6373, 2013

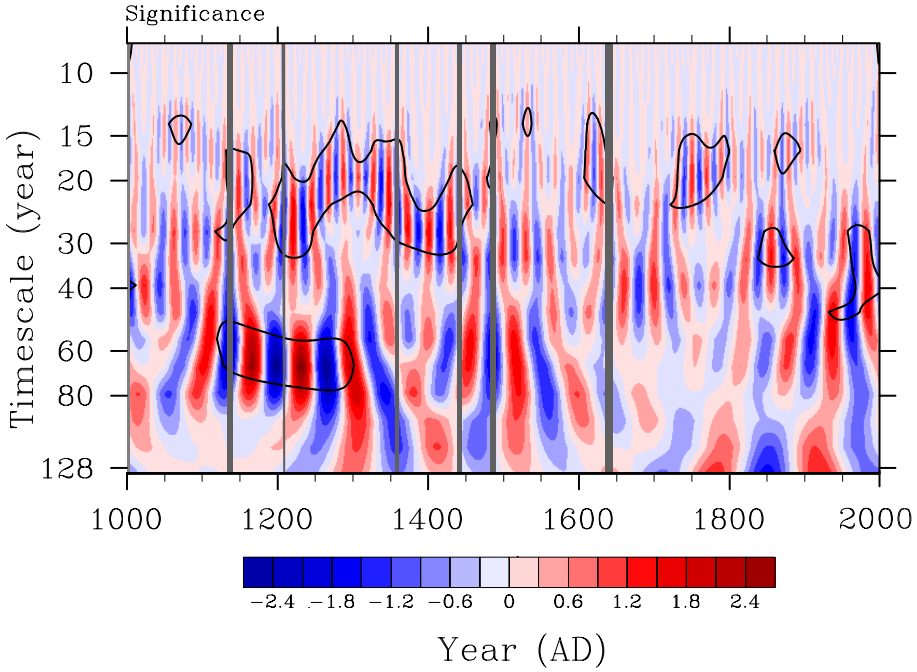

Fig. 5. The real-part coefficients of wavelet transform of the simulate precipitation series. The thick contour encloses regions of greater than 95 % confidence of wavelet power. Six well-captured severe decadal droughts are shown with gray bars.

CPD
9, 6345–6373, 2013

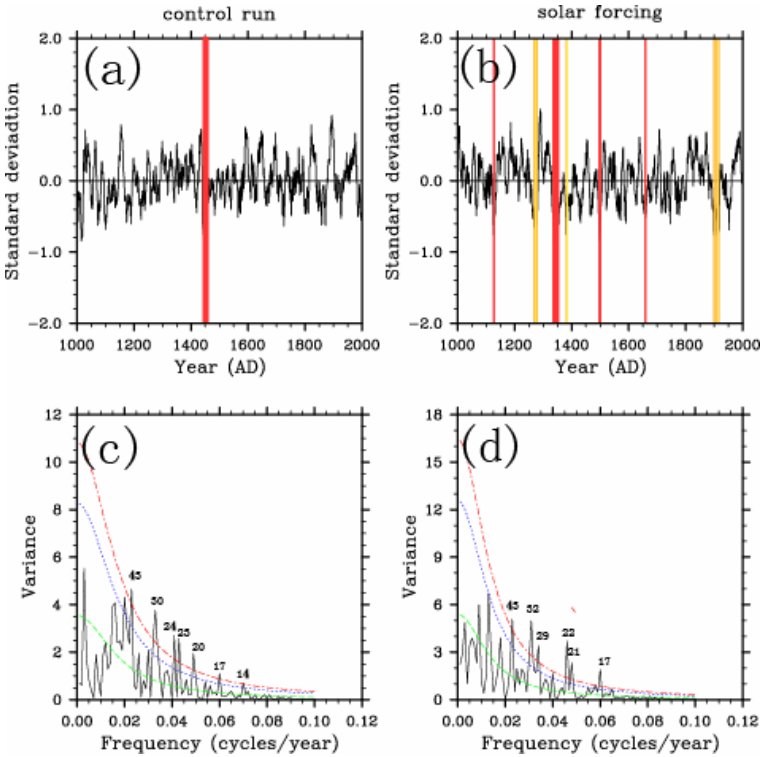

Fig. 6. The 10 yr running mean time series of standardized anomaly variations of summer precipitation rate derived from the control run **(a)** and solar forcing run **(b)**, and the corresponding spectra in the control run **(c)** and solar forcing run **(d)**. The statistical significance of the spectral peaks was tested against the red noise spectrum at the 95 % (red dashed line), 90 % (blue dashed line), and 50 % (green dashed line) confidence levels. The severe droughts in the solar forcing run are shown with shaded bars, and those that are also observed in the full forcing run are shown with red bars.

CPD
9, 6345–6373, 2013

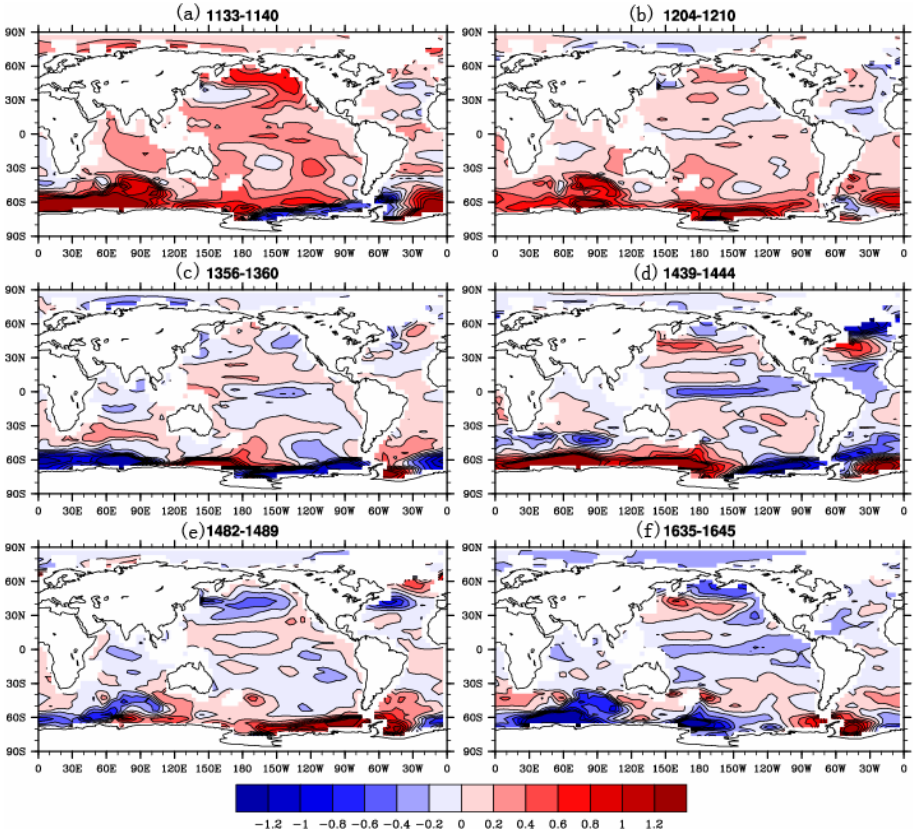

Fig. 7. Same as Fig. 2 but for the global sea surface temperature pattern of the six well-captured droughts.

CPD
9, 6345–6373, 2013

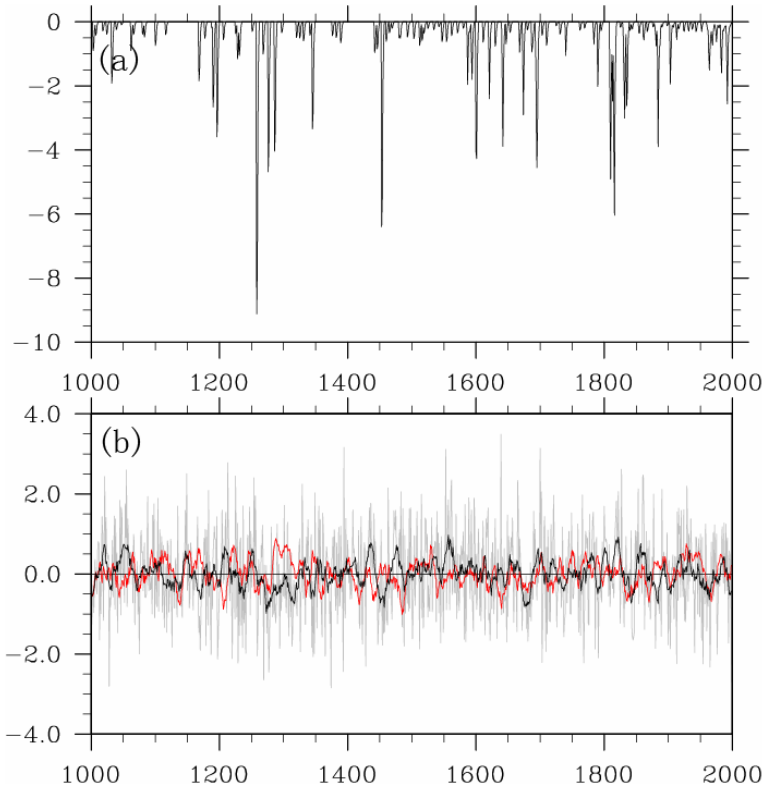

Fig. 8. Volcanic forcing series used by the model shown in W m^{-2} **(a)**. Time series of standardized anomaly variations of summer precipitation rate derived from the volcanic forcing run **(b)**. Black curve represents 10 yr smoothed response. Red curve represents the 10 yr running mean time series of standardized anomaly variations of summer precipitation rate derived from the full forcing run.

CPD
9, 6345–6373, 2013